Noninvasive Skin Hydration Prediction: A Comparison Between Traditional Machine Learning Classifiers and a 1D Convolutional Neural Network

M. R. Rosdi[1,2], A. Huong[2*], X. Ngu[2]
[1] Radibems (M) Sdn Bhd., Hospital Selayang, Batu Caves, 68100, Malaysia
[2]Faculty of Electrical and Electronic Engineering, Universiti Tun Hussein Onn Malaysia, Parit Raja, 86400, Malaysia
[*]corresponding author's email: audrey@uthm.edu.my

Abstract – *Noninvasive monitoring of skin hydration is important for improving the quality of aesthetic care through cost-effective and real-time diagnosis. Existing skin hydration detection systems are expensive, and the process depends heavily on the operator's skills and experience. This paper explored the use of four traditional machine learning classifiers, i.e., K-Nearest Neighbor (KNN), Support Vector Machine (SVM), Decision Tree (DT), and Naïve Bayes (NB), for skin hydration detection using intensity signals produced by a developed two-wavelength near-infrared (NIR) optical system. The performance of these classifiers was compared with that of a one-dimensional convolutional neural network (1D-CNN) designed and optimized for skin hydration classification using data collected from seventeen healthy adult volunteers. The 9-fold cross-validation results demonstrated superior classification performance by the 1D-CNN, achieving an accuracy of 0.677 and other performance metrics ranging from 0.61 to 0.83. These values represent improvements of 1.2 to 2.6 times over traditional classifiers. The poorer performance of the traditional classifiers was attributed to the strong dependence of reflectance at 1200 nm on skin pigmentation. The prediction performance of the proposed system could be further improved by integrating ensemble techniques with deep learning models to extract more discriminative features for analysis.*

Keywords: *classifier, Convolutional Neural Network; K-Nearest Neighbor, near-infrared, skin hydration*

Article History
Received 29 May 2026
Received in revised form 19 June 2026
Accepted 19 July 2026

I. Introduction

Skin moisture plays a vital role in dermatology and cosmetic research. The water-retention capacity of the outer skin layers is crucial for maintaining skin elasticity, thereby influencing overall skin health and appearance. Inadequate water content disrupts the natural shedding process, leading to dry, flaky, compromised skin. A proper balance between skin hydration (moisture) and sebum (skin surface lipids) is essential for safeguarding and maintaining skin integrity [1]-[2]. It has been reported that the skin's water content is notably high in the viable epidermis, comprising approximately 70% water, and significantly diminishes at the junction between the stratum granulosum (SG) and the stratum corneum (SC), where it ranges from 15 to 30% [3].

Near-infrared (NIR) technology is an imaging technique that allows direct measurement of water absorption in human skin via reflectance spectroscopy. NIR spectral data spanning 800-2400 nm have been shown to correlate strongly with skin hydration levels [4]-[5]. They can be used to directly and precisely identify skin hydration by analyzing the intensities of overtone bands and of water-related oxygen-hydrogen (O-H) and water molecular (H-O-H) vibrational bands. The O-H bands of water showcase five absorption peaks within the NIR region: 760 nm, 970 nm, 1190 nm, 1450 nm, and 1940 nm [4]-[6]. Martin [7] applied diffuse reflectance NIR spectroscopy to investigate the effectiveness of moisturizing formulations. A similar study [8] was conducted to estimate the effects of skin moisturizers and cleansers on skin hydration. The results were further compared with the standard electrical methods i.e., conductance and capacitance measurements. NIR was shown to exhibit higher sensitivity in detecting different degrees of hydration and changes in skin hydration induced by skin moisturizers and cleansers. Another study by Wu et al. [9] developed an NIR imaging system for measuring skin hydration; the

This is an Open Access article distributed under the terms of the Creative Commons Attribution 4.0 International License, permitting copy and redistribution of the material and adaptation for commercial and uncommercial use.

results were compared with those of the Corneometer and Skicon-200EX, which are commonly used instruments for evaluation. The findings were compared before application and at 15 min and 60 min after application. Instead of using a bulky, complex imaging system, Shen et al. [10] demonstrated the use of a miniature NIR spectrometer for in vivo evaluation of five commercially available moisturizing products. The findings suggested that a detection distance of 1 mm was optimal and concluded that the 1750-2150 nm wavelength range was the most suitable wavelength range for the evaluation. A dual-wavelength wearable NIR device using wavelengths 970 and 1450 nm was explored in [11] for noncontinuous monitoring of skin hydration and body sweat loss. Instead of the NIR range, Chen et al. [12] explored visible wavelengths (400-1000 nm) to quantify skin absorption and scattering modulation to changes in skin hydration. Changes in the scattering coefficient have been reported to be useful for evaluating cellular thickening and swelling following the accumulation of water in the skin's intracellular spaces.

Although earlier studies [8]-]9] showed that skin hydration assessment can be sufficiently performed by measuring changes in NIR intensities relative to baseline, i.e. NIR scores, artificial intelligence (AI) is a popular technology that can also be used for this task. Machine learning (ML) is one of the earliest AI methods that allows computers to learn from and analyze data without explicit programming. Reference [12] proposed using a two-layer photon diffusion model and a least-squares fitting algorithm for the estimation of skin hydration-related optical properties. This handcrafted method, however, required extensive programming and prior knowledge in model design. Various supervised ML algorithms are available and widely used with the NIR technique to quantify different skin optical properties, such as blood glucose levels [13] and melanin content [14]. These ML methods include K-Nearest Neighbor (KNN), Support Vector Machine (SVM), Decision Tree (DT), Naïve Bayes (NB), Discriminant Analysis (DA), Random Forest (RF), Extreme Gradient Boosting (XGBoost) and Regression techniques for similar classification tasks. Volkova et al. [11] used the LightGBM model, a tree-based learning algorithm, to predict skin hydration. Similarly, [10] proposed using principal component analysis (PCA) for feature extraction and dimensionality reduction as an alternative data analysis method for skin surface moisture detection, thus simplifying the complex relationship between the NIR spectrum and skin properties.

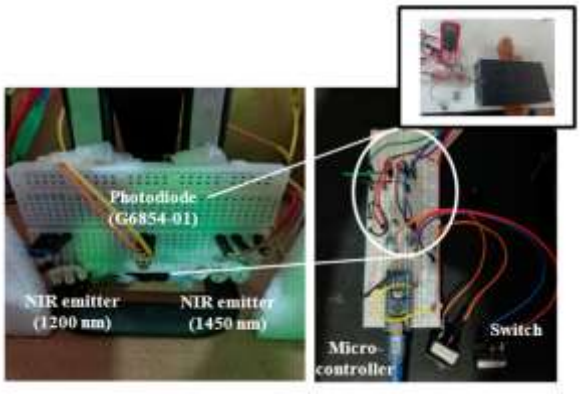
Deep learning (DL) is a branch of ML that uses algorithms inspired by the human brain, known as artificial neural networks. These networks consist of multiple layers, allowing computers to recognize complex patterns in large datasets. Previous research in [15] showed that DL, particularly convolutional neural networks (CNNs), has had a substantial impact across a range of applications, including medical image analysis tasks such as tumor detection and pathology identification. Nonetheless, to the best of our knowledge, this method has not been investigated with NIR technology in skin hydration prediction. It is expected that the combined use of ML and DL with the NIR spectroscopy developed in this study may enable real-time, objective measurements of skin hydration levels. The objective of this paper is to investigate and compare the performance of well-known ML classifiers and a 1D CNN customized for skin hydration prediction using NIR signals.

II. Experimental System, Data Handling and Processing

This paper proposes an NIR prototype for reflectance-based light-intensity measurement. The following describes the developed system, incorporating an NIR prototype and different analytical methods, for noncontact, portable, and real-time skin hydration monitoring. The following subsections also describe human subjects' recruitment, data collection, and processing.

A. NIR Measurement Device

Fig. 1 shows the optical device designed for measuring skin hydration measurement. The system, as shown on the left of the figure, used three NIR photodiodes for each of the two wavelengths employed (1200 and 1450 nm), arranged on the left and right, respectively, of the InGaAs sensor (center). These wavelengths are among the strong water absorption bands across different skin regions in Fig. 2, as published in [16]. The optical components are positioned at 1.5 cm and 45°, perpendicular to the skin surface. These arrangements were decided based on the detected light intensities. Separate switches (shown on the right in Fig. 1) were used to concurrently and independently turn on the 1200 and 1450 nm sources during data acquisition. The sensor was connected to a digital multimeter to measure the voltage generated by the light signal reflected from the skin surface during the experiment.



(a) (b)

Fig. 1. (a) Optical arrangement of light sources and detector (b) functioning and controlling of the optical system. The right inlet shows an image taken during data collection

The circuit in Fig. 1 was enclosed in a makeshift dark chamber, as shown in the top-right inset of the figure. A small hollow opening in the chamber, with approximate dimensions of 8 cm × 12 cm, was created for arm placement during data collection, hence minimizing background interference from surrounding environmental light sources.

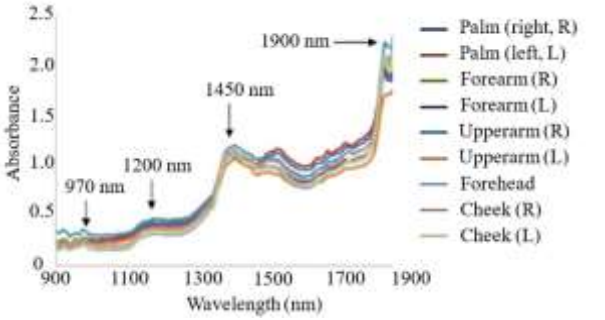


Fig. 2. Near-infrared (NIR) water absorbance spectra of different human skin sites measured over the wavelength range of 900-1900 nm

B. Human Subjects, Experimental Method, and Data Collection

This study recruited seventeen participants (n = 17), all males aged 18 to 36, to test the system's performance after obtaining approval from the Human Research Ethics Committee (HREC) of Universiti Tun Hussein Onn Malaysia (Ref no. RMC.100-9/39(22)). The participants were briefed on the experimental method and provided written consent before participating in the study. Measurement was collected from the midpoint of the anterior and posterior regions of their lower right arm. The skin color characteristics of the participants characterized based on Fitzpatrick scale were as follows: skin color type II (n = 6), III (n = 3), IV (n = 6), and V (n = 2) for anterior and type II (n = 1), III (n = 4), IV (n = 4), and V (n = 8) for the posterior skin.

This paper collects reflectance measurements from these sites under three experimental conditions: (1) clean and dry skin, which served as the baseline, (2) immediately following moisturizer application, and (3) 15 min post-application, as shown in Fig. 3. Since the proposed system employs a multimeter to measure the photodetector output, each acquisition consists of a single steady-state voltage value representing the reflectance measurement. The topical moisturizer used for the measurement was cream by Derma Health's SkinLabs. A pea-sized amount of the cream was applied to the anterior forearm after the selected site was cleansed and patted dry. Three measurements were collected under each condition, and their average was used as the representative signal for that condition. Another set of three measurements was collected 15 minutes after the moisturizer was applied, and the average of these measurements was similarly used as the representative signal. The same procedure was repeated for the posterior forearm.

The 102 samples, corresponding to data collected from 17 subjects × 2 sites × 3 experimental conditions, at each light wavelength, were imported into MATLAB for processing.



Fig 3. Experimental conditions and data collection flow

III. Prediction Models and Performance Analysis

The following subsections discuss four traditional ML classification models and a 1D CNN model designed for three-class skin hydration classification. The raw data collected from the experiments in Fig. 3 were averaged and annotated according to their moisture category (i.e., dry, moisturized, and hydrated). No other signal processing operation was applied. The input features, i.e. two-column intensity signals of the considered light wavelengths and the label array Y, i.e. classes C_0 (dry), C_1 (immediately after moisturizer application), and C_2 (15 min post-application), are arranged and used to train the ML and DL models. These signals were split into training and test sets for training the ML and CNN models using k-fold validation. The investigation of optimum k-fold value is by varying the number of folds (k-fold) from 2 to 20, as summarized in Fig. 4, using the performance of ML classifiers as the benchmark due to their comparatively low computational demands.

A. Traditional Machine Learning (ML) Classifiers

Four traditional ML classifiers, specifically KNN, SVM, DT and NB models were considered in this research because they can be readily applied using MATLAB toolboxes. The KNN implementation was using the *fitcknn* function in MATLAB. The number of neighbors was arbitrarily chosen as 10 for demonstration. Meanwhile, the SVM model was trained using the *fitcecoc* function, which applies the Error-Correcting Output Codes (ECOC) framework to extend binary SVM classifiers to multi-class problems. The DT classifier, which recursively splits the dataset into smaller, more homogeneous groups, was implemented using the *fitctree* function, whereas the NB model's decision rule was fine-tuned using the *fitcnb* function in MATLAB.

After cross-validation training, the trained models were used to generate predictions for the validation folds using the *kfoldPredict* function. These predicted labels were compared with the ground truth labels (Y) to

produce a confusion matrix and evaluate performance metrics.

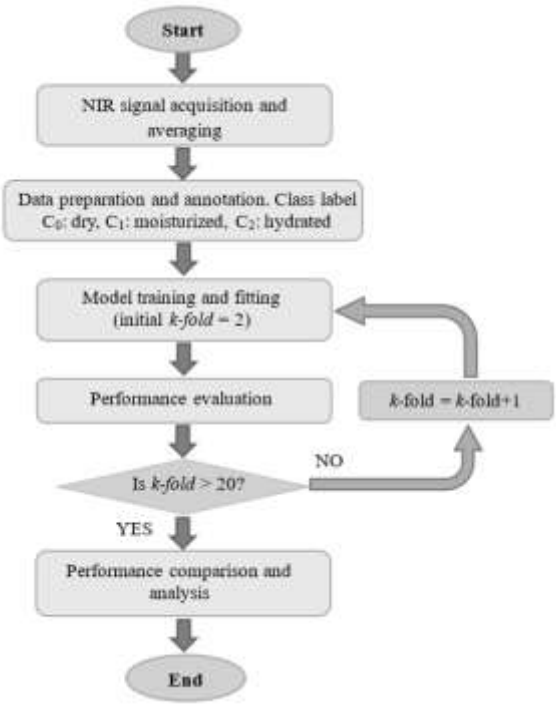


Fig. 4. Data handling and machine learning model training workflow and sensitivity analysis

B. 1D CNN Model

In addition to the classifiers discussed in the earlier section, this study designed a 1D CNN model based on the framework published in one of our early works [17]. This model comprises of four convolutional layers as shown in Fig. 5. This architecture is selected following iterative evaluation of models with one to six convolutional layers, as it provided the best classification performance while maintaining a simple and computationally efficient architecture. Features extracted by the convolutional blocks were fed into batch normalization to help regulate the outputs before they were passed to the activation layer. A pooling layer was placed after every two convolutional blocks to reduce dimensionality and hence minimize model overfitting.

This paper optimizes the network architecture parameters using a grid search, with candidate filter and pooling sizes listed in Table I, based on the ranges adopted from [17]. In addition, the learner type (L), mini-batch number (β), and initial learning rate (γ), whose ranges are also presented in Table I, were fine-tuned to improve the model's generalizability. This optimization process involved evaluating 324 possible parameter combinations, as listed in the table. Each combination was tested before the optimal model was selected based on the highest mean training and validation accuracies achieved.

TABLE I
THE 1D CNN MODEL DESIGN PARAMETERS AND THEIR SEARCH RANGE

Element	Parameters	Possible Solution
Networlayers (Conv. 1 - 4	Filter size, N	{10, 20, 30}
Network layers (Pool 1 and 2)	MaxPooling size ψ	{10, 20, 30}
Training hyperparameter	Learner type L	1→3: {*Adam*, *Sgdm*, *RMSProp*}
	Mini-batch no. β	{50, 100, 150, 200}
	Init. Learning rate γ	{0.005, 0.01, 0.05}

C. Performance Metrics

The performance of the considered models, tested using a cross-validation technique, is evaluated using the common metrics shown in (1) to (5). Classification accuracy is the ratio of correctly predicted samples, across both positive and negative classes, to the total number of samples. Precision in (2) indicates the reliability of the model's positive predictions. Sensitivity, also known as recall in (3), measures the model's ability to correctly detect positive instances, while specificity evaluates its ability to identify negative instances correctly. Meanwhile, the F1-score represents the harmonic mean between precision and sensitivity.

$$Accuracy = \frac{TP+TN}{TP+FP+TN+FN} \quad (1)$$

$$Precision = \frac{TP}{TP+FP} \quad (2)$$

$$Sensitivity = \frac{TP}{TP+FN} \quad (3)$$

$$Specificity = \frac{TN}{TN+FP} \quad (4)$$

$$F1 = \frac{2\,(Prec * Sens)}{Prec+Sens} \quad (5)$$

True positive (TP) and true negative (TN) denote instances that the model correctly classified as positive and negative, respectively. In contrast, false positives (FPs) and false negatives (FNs) correspond to incorrect classifications made by the model. Statistical analysis is also carried out to evaluate differences in the measured signals in relation to the skin color using a one-way ANOVA in SPSS version 23.0 with a significance threshold of $\sigma = 0.05$.

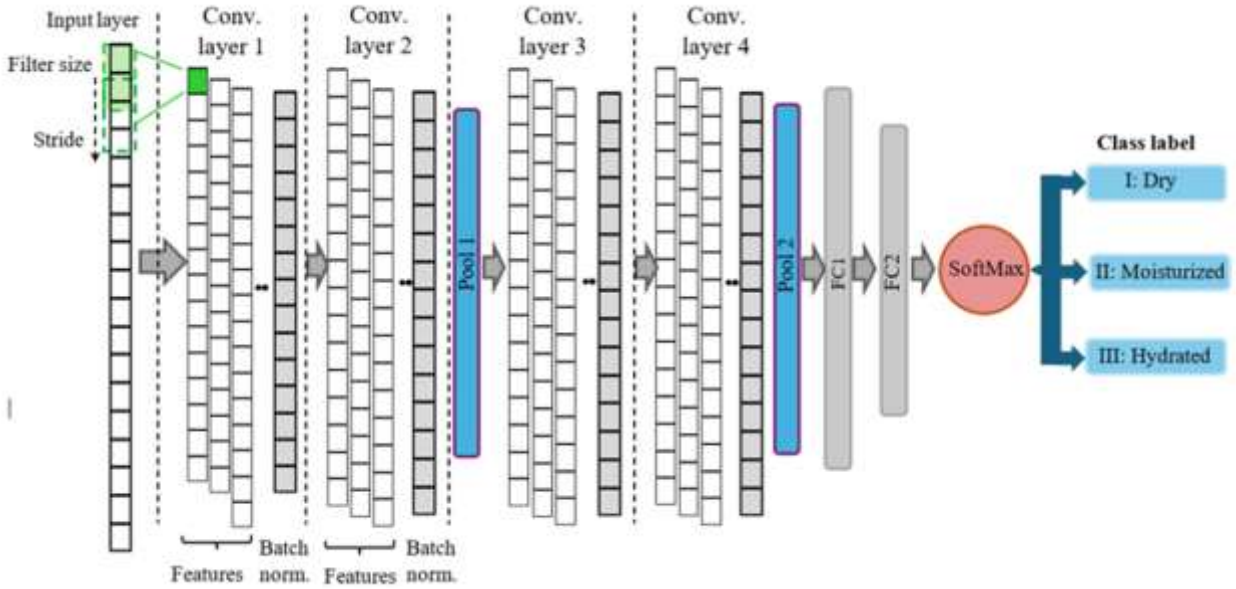


Fig. 5. The proposed 1D convolutional neural network (CNN) architecture

IV. Results and Analysis

Our experimental results demonstrate acceptable magnitudes of reflected light intensity. A larger difference was also observed between the signal magnitudes recorded under illumination at 1200 and 1450 nm, as shown in Fig. 6, consistent with the water absorbance in Fig. 2. The relatively large signal magnitudes are desirable, as they improve measurement sensitivity and facilitate more reliable analysis. Nonetheless, our investigation showed negligible differences among the skin hydration conditions, with mean values (bar height) ranging from 6.38 to 6.60 V and 1.60 to 1.65 V under the two illumination wavelengths. Their standard deviations, represented by the error bars, further indicate that the signal magnitude ranges were highly consistent across all experimental conditions, with only minimal variation between hydration states. These subtle nonlinear variations may not be adequately captured by traditional statistical analyses, which primarily evaluate linear relationships and univariate differences between groups. Therefore, ML and DL models are employed to automatically extract and learn these latent features, enabling effective differentiation between conditions that exhibit highly similar statistical characteristics.

Given the small differences between the conditions, the robustness and generalizability of the models employed were further evaluated by varying the number of folds (k) in k-fold cross-validation. The ML models were adopted as benchmarks due to their relatively lower representational capacity and generally poorer ability to generalize complex nonlinear patterns compared with the DL model. A sensitivity analysis was performed by varying k-fold from 2 to 20 with a step size of 1 to determine the optimal k-fold values for training and validation of the ML classifiers (i.e., KNN, SVM, Decision Tree, and Naïve Bayes). The testing accuracy of the models at each iterative k-fold value was recorded. The mean accuracy was calculated by averaging across classifiers, as shown in Fig. 7. Based on these results, a k-fold value of 9 was identified as the optimal data-splitting ratio for producing trained models with good generalization. Therefore, the cross-validation results for the models trained with this k-fold value were recorded and plotted in Fig. 8. The confusion matrices were used to compute the evaluation metrics shown in Table II.

For fair comparison, the CNN model in Fig. 5 was trained, validated, and tested using 9-fold cross-validation. The iterative training and validation of the model identified *Sgdm* as the best learner type, the optimal minibatch size, $\beta = 150$, and the initial learning rate $\gamma = 0.005$. The best network filter size and pooling size are identified as 20. This design yields a 19-layer model with 89,000 learnable parameters. The model trained using these training and network parameters is tested, producing a confusion matrix shown in Fig. 9. Based on this table, the performance metrics are calculated and tabulated in Table II.

Meanwhile, the ANOVA test revealed no relationship between the measurements at 1450 nm and skin color ($\rho = 0.173$). However, a strong correlation exists between the 1200 nm data and the subjects' skin pigmentation ($\rho = .000$).

This is an Open Access article distributed under the terms of the Creative Commons Attribution 4.0 International License, permitting copy and redistribution of the material and adaptation for commercial and uncommercial use.

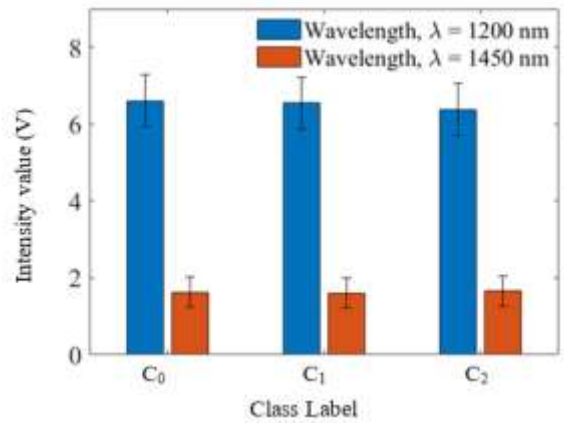


Fig. 6. The mean (bar height) and standard deviation (error bar) of intensity data calculated from measurements of seventeen recruits for measurement under dry (C_0), moisturized (C_1), and hydrated conditions (C_2), and under 1200 and 1400 nm

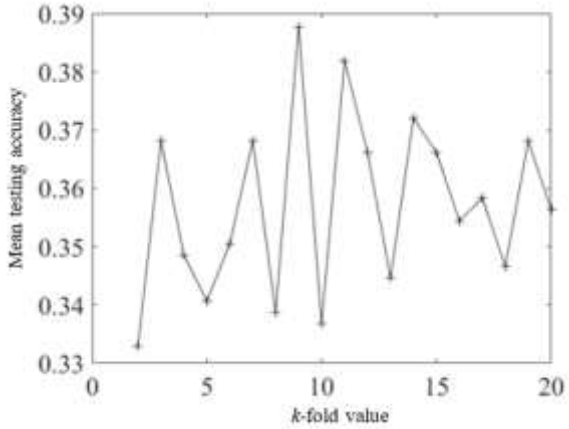


Fig. 7. Mean testing accuracy across different *k*-fold values from 2 to 20. The mean represents the average testing performance of the four traditional machine learning classifiers considered

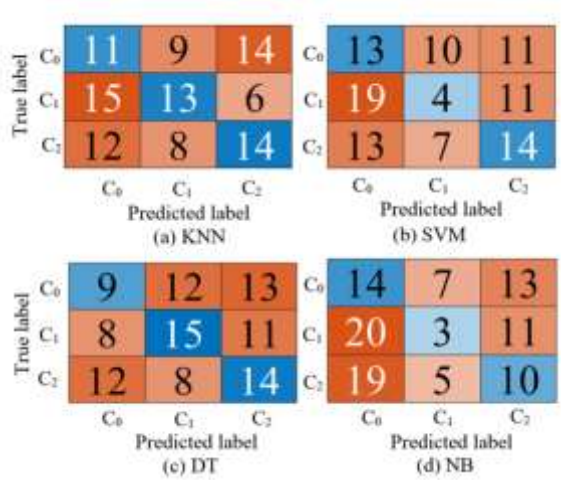


Fig. 8. The confusion matrix of (a) K-Nearest Neighbor (KNN), (b) Support vector machine (SVM), (c) Decision Tree (DT) and (d) Naïve Bayes (NB) trained and cross-validated with 9-fold using reflectance data at wavelength, λ, 1200 and 1450 nm. Class label C_0: Dry, C_1: Moisturized, and C_2: Hydrated conditions

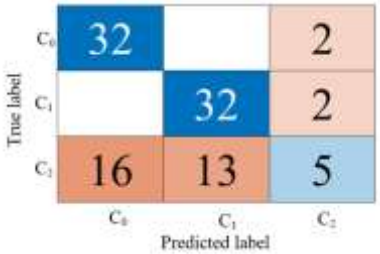


Fig. 9. Confusion matrix of 1D CNN evaluated using 9-fold cross-validation. Class label C_0: Dry, C_1: Moisturized, and C_2: Hydrated conditions

TABLE II
COMPARISON OF THE PERFORMANCE METRICS OF THE CONSIDERED MODELS TRAINED AND TESTED USING RAW MEASUREMENT DATA

Metrics	Prediction Models				
	KNN	SVM	DT	NB	1D CNN
ACC	0.3725	0.3039	0.3725	0.2647	0.6765
PREC	0.3782	0.2894	0.3691	0.2528	0.6444
SENS	0.3725	0.3039	0.3725	0.2647	0.6765
SPEC	0.6863	0.6520	0.6863	0.6324	0.8382
F1	0.3745	0.2915	0.3698	0.2461	0.6077

ACC:accuracy,PREC:precision,SENS:sensitivity,SPEC:specificity, NB:Naïve Bayes

V. Discussion

This paper explores and compares the performance of ML and DL methods for classifying skin hydration using intensity data from the developed dual-wavelength optical system. This study observed negligible differences in the wavelength-dependent magnitudes of the reflected signals, as shown in Fig. 6. The statistical test showed no difference between the measurements (ρ>0.05). These occluded points hinder the traditional ML classifiers from adeptly capturing the intricate patterns in the data. Table II shows considerably lower metric values for these classifiers, ranging from 0.2 to 0.69. On the contrary, the proposed 1D-CNN, designed to learn the complex features of the dataset used, outperformed its traditional ML counterparts by about 1.2-2.6 times, depending on the metrics evaluated in the table.

Although ML classifiers performed poorly, with negligible differences in performance metrics, particularly between the decision tree and KNN models, the Naïve Bayes classifier achieved the lowest accuracy of 0.265, while the remaining performance metrics ranged from 0.25 to 0.63. Despite the distinct water absorption characteristics observed at different wavelengths in Fig. 2, the results in Fig. 6 reveal a high degree of similarity in the magnitudes of the spectral signals across the experimental conditions. This suggests that the discriminative information is embedded within small nonlinear spectral variations rather than

pronounced differences in signal intensity. Such high inter-class similarity reduces feature separability and poses a significant challenge for conventional ML classifiers. Unlike KNN, SVM, and decision trees, which adapt to the dataset's features without using a parametric model, Naïve Bayes assigns prior probabilities to each class based on the input data. Thus, the results in Table II suggest that the class probabilities for the target variables may be too similar, leading to poor model fit.

In addition, optical measurements were conducted on the subjects' anterior and posterior forearms to assess the system's robustness. The statistical results indicated a positive correlation (ρ = 0.000) between the Fitzpatrick scale and the reflectance signal, especially at 1200 nm. Therefore, skin pigmentation, combined with low sampling resolution, could contribute to reduced discrimination in the feature subspace, especially with traditional classifiers. The lightweight 1D CNN, with 89,000 learnable parameters, uses convolutional layers to extract relevant, complex features from the reflectance data. Although the differences in signal magnitudes between the class labels are small, this model can extract complex nonlinear relationships and feature interactions across different wavelengths and identify latent discriminative patterns that are not adequately captured by conventional ML methods, outperforming its traditional counterparts with an overall accuracy of 0.677.

Figure 9 showed that this model achieved a near-perfect score for detecting dry and moisturized skin conditions, with a higher precision of 0.644. The confusion chart in Fig. 9 showed that 29 samples from the hydrated condition were misclassified into the dry and moisturized classes, increasing the *FN* rate and, hence, lowering the model's sensitivity to 0.677. The findings of this study suggest that overlapping values between the hydrated and other experimental conditions may contribute to the increased misclassification rate. It is expected that this model's performance can be improved by increasing network depth to enhance feature extraction, increasing the number of instances per class, or exploring and fine-tuning other network design parameters to optimize data training.

Since the proposed 1D CNN was shown to extract important features useful for classification tasks, future work in this direction includes incorporating ML classifiers into the CNN model to improve the system's discriminative power in decision-making. This study excludes female participants to minimize the effects of gender differences in skin thickness and biophysical properties. Future studies will also include recruiting female participants and a larger, more diverse population. In addition, adopting a longer NIR light wavelength, i.e., 1900 nm, whose water absorption is higher than that at 1200 and 1450 nm, would be more appropriate. This wavelength is unaffected by pigmentation due to the reduced melanin absorption at wavelengths deeper in the NIR region. Other possible efforts also include optimizing the optical sensing configuration, feature selection techniques, and advanced deep learning architectures that may further enhance the overall system performance.

VI. Conclusion

This study presents an AI-integrated optical system for noninvasive, real-time monitoring of skin hydration. The measured reflectance data were used for prediction using KNN, SVM, decision tree, and Naïve Bayes classifiers, and the results were compared with those of a lightweight 1D-CNN model customized and optimized for the problem. The results showed the superior performance of the deep learning CNN compared to traditional counterparts, achieving an overall classification accuracy of 0.677. This study recommended combining CNNs and ML classifiers in future classification research to improve the model's discriminative capability and classification accuracy.

Acknowledgements

This research was supported by the Ministry of Higher Education (MOHE) through the Fundamental Research Grant Scheme (FRGS) (FRGS/1/2024/TK07/ UTHM/02/5) and Universiti Tun Hussein Onn Malaysia (UTHM) through GPPS (vot H659).

Conflict of Interest

The authors declare no conflict of interest in the publication process of the research article.

Author Contributions

The authors confirm contribution to the paper as follows: study conception and design: A. Huong, X. Ngu; data collection: M.R. Rosdi; analysis and interpretation of results: A. Huong, M.R. Rosdi; draft manuscript preparation: M.R. Rosdi, A. Huong; review and editing: A. Huong, X. Ngu. All authors reviewed the results and approved the final version of the manuscript.

References

[1] S. F. Bernatchez and J. Bichel, "The science of skin: Measuring damage and assessing risk," *Wounds*, Apr. 2023, doi: 10.1089/wound.2022.0021.

[2] D. Li et al., "A comprehensive review: The bidirectional role of sebum in skin health," *Bioengineering*, vol. 12, no. 12, Dec. 2025, Art. no. 1333, doi: 10.3390/bioengineering12121333.

[3] D. Lunter, V. Klang, D. Kocsis, Z. Varga-Medveczky, S. Berkó, and F. Erdő, "Novel aspects of Raman spectroscopy in skin

research," *Exp. Dermatol.*, vol. 31, no. 9, pp. 1323–1335, Sep. 2022, doi: 10.1111/exd.14645.

[4] M. Egawa, M. Yanai, N. Maruyama, Y. Fukaya, and T. Hirao, "Visualization of water distribution in the facial epidermal layers of skin using high-sensitivity near-infrared (NIR) imaging," *Appl. Spectrosc.*, vol. 69, no. 4, pp. 481–487, Apr. 2015, doi: 10.1366/14-07571R.

[5] A. Mancuso, N. d'Avanzo, M. C. Cristiano, and D. Paolino, "Reflectance spectroscopy: A non-invasive strategy to explore skin reactions to topical products," *Front. Chem.*, vol. 12, 2024, Art. no. 1422616, doi: 10.3389/fchem.2024.1422616.

[6] K. B. Beć and C. W. Huck, "Breakthrough potential in near-infrared spectroscopy: Spectra simulation. A review of recent developments," *Front. Chem.*, vol. 7, 2019, Art. no. 48, doi: 10.3389/fchem.2019.00048.

[7] K. Martin, "In vivo measurements of water in skin by near-infrared reflectance," *Appl. Spectrosc.*, vol. 52, no. 7, pp. 1001–1007, Jul. 1998, doi: 10.1366/0003702981944652.

[8] S. L. Zhang, C. L. Meyers, K. Subramanyan, and T. M. Hancewicz, "Near infrared imaging for measuring and visualizing skin hydration: A comparison with visual assessment and electrical methods," *J. Biomed. Opt.*, vol. 10, no. 3, May/Jun. 2005, Art. no. 031107, doi: 10.1117/1.1922347.

[9] Y. Wu, J. Ran, T. Tanaka, and Q. Liu, "Quantitative skin surface hydration measurement by visible optical image processing: A pilot study," *Skin Res. Technol.*, vol. 30, no. 6, Jun. 2024, Art. no. e13773, doi: 10.1111/srt.13773.

[10] X. Shen, S. Lan, Y. Zhao, Y. Xiong, W. Yang, and Y. Du, "Characterization of skin moisture and evaluation of cosmetic moisturizing properties using miniature near-infrared spectrometer," *Infrared Phys. Technol.*, vol. 132, 2023, Art. no. 104759.

[11] E. Volkova et al., "Multispectral sensor fusion in SmartWatch for in situ continuous monitoring of human skin hydration and body sweat loss," *Sci. Rep.*, vol. 13, no. 1, 2023, Art. no. 13371.

[12] Y. Y. Chen, S. Y. Tzeng, Y. Y. Yen, N. Y. Cheng, and S. H. Tseng, "Non-invasive assessment of skin hydration and sensation with diffuse reflectance spectroscopy," *Sci. Rep.*, vol. 13, no. 1, 2023, Art. no. 20149.

[13] M. Naresh, V. S. Nagaraju, S. Kollem, J. Kumar, and S. Peddakrishna, "Non-invasive glucose prediction and classification using NIR technology with machine learning," *Heliyon*, vol. 10, no. 7, 2024.

[14] L. Wei, X. Yi, W. Cheng, Y. Ma, and Y. Lin, "Hyperspectral imaging combined with machine learning methods to quantify the facial skin melanin and erythema," *J. Biophotonics*, vol. 19, no. 2, 2026, Art. no. e70146.

[15] M. Shoaib et al., "An advanced deep learning models-based plant disease detection: A review of recent research," *Front. Plant Sci.*, vol. 14, 2023, Art. no. 1158933.

[16] Light Absorption by Water. (2017). [Online]. Available: https://omlc.org/spectra/water/

[17] A. Huong, K. G. Tay, K. B. Gan, and X. Ngu, "MI-OPTNET: An optimized deep learning framework for myocardial infarction detection," *J. Teknol.*, vol. 86, no. 3, 2024, doi: 10.11113/jurnalteknologi.v86.20409.